Observation of ultrahigh density InGaN quantum dots

H. L. Tsai, T. Y. Wang, and J. R. Yang[a)]
Institute of Materials Science and Engineering, National Taiwan University, Taipei, Taiwan 106, Republic of China

T. C. Wang and J. T. Hsu
Electronics and Optoelectronics Research Laboratories, Industrial Technology Research Institute, Hsinchu, Taiwan 310, Republic of China

M. Shiojiri[b)]
Kyoto Institute of Technology, Kyoto 606-8585, Japan and Department of Anatomy, Kanazawa Medical University, Ishikawa 920-0293, Japan

(Received 28 December 2006; accepted 30 April 2007; published online 10 July 2007)

High density InGaN quantum dots (QDs) grown on an underlying GaN layer that was partially masked with SiN_x nanocrystals were investigated by cross-sectional high-angle annular dark-field (HAADF) scanning transmission electron microscopy (STEM), high-resolution transmission electron microscopy, and energy dispersive x-ray spectroscopy. The layer of SiN_x masks appeared as a dark line in the HAADF-STEM images, and from the thickness of that dark line, the height of the masks was roughly estimated to be less than 2 nm. The InGaN QDs appeared as bright triangles in the HAADF-STEM images. The QDs can be regarded as nanosized island crystals consisting of $\{10\bar{1}1\}$ sidewalls, with a height of several nanometers. The lattices in the InGaN crystals were strained as compared to the underlying and the capping GaN lattices and contacted them coherently. © *2007 American Institute of Physics*. [DOI: 10.1063/1.2745848]

I. INTRODUCTION

Violet or purple light emitting diodes (LEDs) and laser diodes (LDs) with multiple InGaN/GaN quantum well (QW) structures are widely manufactured for commercial use. It has been proposed that In-rich clusters, which act as quantum dots (QDs) in the InGaN QWs, are the origin of the high emission efficiency in InGaN-based LEDs and LDs.[1–5] Via atomic-resolution high-angle annular dark-field (HAADF) scanning transmission electron microscopy (STEM) maps, which provide both precise atom column positions and the atomic number dependent contrast (*Z* contrast), strained lattices have been observed in In-rich clusters.[6] Carriers that are deeply localized in QDs are hindered from migrating toward dislocations.[7] The resulting photoluminescence (PL) is surprisingly unaffected by the numerous dislocations. The performance of LDs is expected to be greatly improved if the density of QDs can be made to far exceed that of dislocations. Structures of the active layer with QDs, instead of QWs, have been pursued.[8–15] One approach to fabricating InGaN QDs is to deposit silicon antisurfactant or SiN_x nanomasks, which alter the morphology of the AlGaN films from that of step flow to that of a three-dimensional island, facilitating the formation of GaN QDs (Ref. 16) and InGaN QDs (Ref. 9) on the AlGaN. Recently, Tu *et al.*[17] reported that an ultrahigh density of InGaN QDs of $\sim 3\times 10^{11}$ cm^{-2} was obtained using a SiN_x nanomask. Their InGaN QDs exhibited strong PL emission at room temperature (RT). Increasing the duration of the SiN_x treatment on the underlying GaN layer provided a redshift of the RT-PL peak from violet to green and broadened the spectrum.

There have been very few structural investigations of the AlGaN QDs other than atomic force microscopy (AFM) observations. This paper reports on our electron microscopy (EM) analysis of InGaN QDs conducted with high-resolution transmission electron microscopy (HRTEM), HAADF-STEM, and energy dispersive x-ray spectroscopy (EDX).

II. EXPERIMENTAL PROCEDURE

The sample was similar to that used in the previous experiment by Tu *et al.*[17] and prepared by metal organic vapor phase epitaxy (MOVPE). The structure is schematically shown in Fig. 1. A GaN nucleation layer 30 nm thick was grown at a low temperature (LT) of 550 °C on the (0001) sapphire substrate. An *n*-GaN:Si underlying layer 2 μm

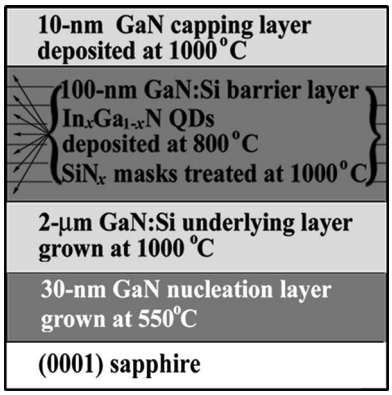

FIG. 1. Structure of the sample used in the present experiment.

a)Author to whom correspondence should be addressed; electronic mail: jryang@ntu.edu.tw
b)Present address: 1-297 Wakiyama, Enmyoji, Kyoto 618-0091, Japan; electronic mail: shiojiri@pc4.so-net.ne.jp

thick was deposited on the nucleation layer at a reactor temperature of 1000 °C to produce a step flow grown surface. This underlying GaN layer was then masked with a rough SiN_x layer, followed by the deposition of the QDs. The treatment of the SiN_x was performed at flow rates of 5 slm (standard liters per minute) for NH_3 and 50 SCCM (SCCM denotes cubic centimeter per minute at STP) for diluted Si_2H_6. The reactor temperature was then lowered to 800 °C for the deposition of the $In_xGa_{1-x}N$ QD layer. The deposition of a pair of the SiN_x and InGaN layers was repeated using a spacer of a 100 nm GaN:Si barrier layer deposited at 1000 °C, and finally the last InGaN layer was capped with an undoped GaN layer 10 nm thick deposited at 1000 °C. All the layer thicknesses shown above are nominal values.

The specimens for cross-sectional EM nanoanalysis were prepared by mechanical polishing, followed by ion milling. HAADF-STEM, HRTEM, and qualitative EDX nanoanalysis were performed in a Tecnai 30 equipped with a lens of $C_s=1.2$ mm and operated at 300 keV. The HAADF-STEM images were recorded in a detector range of $D=36-181$ mrad using a convergent electron probe with a semiangle of $\alpha=15$ mrad. All the HAADF-STEM and HRTEM images presented in this paper are raw images, free of any image processing.

III. RESULTS AND DISCUSSION

Tu *et al.*,[17] who performed AFM observations of samples similar to the present one, reported that a flat InGaN layer with a slightly rough layer of 20 monolayer islands formed on the GaN without any SiN_x treatment and that three-dimensional growth of InGaN occurred on GaN treated with SiN_x. This led them to conclude that the formation of InGaN QDs can be controlled by changing the duration of the SiN_x treatment. The evaluated average height and dot density of the QDs increased from 3.6 to 4.1 nm and from 2.1×10^{11} to 2.9×10^{11} cm^{-2} when the duration of the SiN_x treatment was increased from 390 to 420 s, which explains the redshift of the RT-PL peak. However, they did not perform any analysis of the SiN_x layer. They assumed the existence of the SiN_x layer from the results they found, that the growth of the InGaN dots was influenced by the duration of the SiN_x treatment and that when the duration of the SiN_x treatment was increased, the GaN/InGaN dots did not grow (as the SiN film must have covered the underlying layer entirely).

Figure 2(a) shows a low magnified HAADF-STEM image of the specimen. The dark area in the upper right corner can be disregarded, that is, where epoxy resin used for the EM sample preparation was placed. EDX analysis was performed using a probe size of ~0.5 nm along the line indicated in Fig. 2(a), which was a detecting area with a width of ~1 nm. The line is parallel to the edge of the specimen, or the basal plane of the GaN, settled just above a SiN_x layer (which is described below and in Fig. 4). Figure 2(b) shows the HAADF-STEM intensity profile along the line in Fig. 2(a). Figure 2(c) reproduces the averaged EDX spectrum acquired from that line. A weak emission from Si was detected together with a very strong emission from In and strong

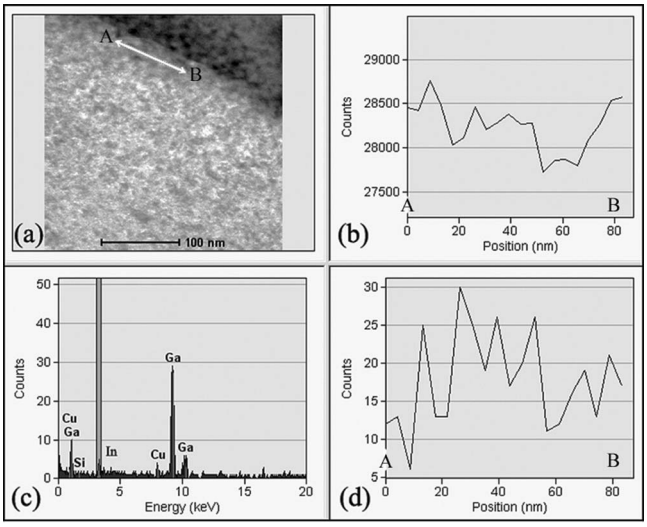

FIG. 2. (a) HAADF-STEM image in which the area line scanned for EDX is indicated. (b) HAADF-STEM intensity profile along the line *A*-*B* shown in (a). (c) EDX spectrum. (d) Indium L_β intensity profile along the line *A*-*B* in (a).

emissions from Ga. The signal for Cu originated from the specimen support. EDX analysis proves the existence of Si, which was used to form the masks. Figure 2(d) shows the intensity profile of In-L_β along the line. HAADF-STEM images give rise to strong contrast dependence on the atomic number *Z* contrast, unlike conventional TEM images, since they are mainly formed by thermal diffuse scattering of electrons or incoherent imaging of elastically scattered electrons.[18,19] Therefore, according to the high thermal diffuse scattering cross section of In[49] atoms compared with Ga[31] atoms, the HAADF-STEM intensity of the InGaN is stronger than that of the GaN. In any case, the intensity of the SiN_x is the weakest, regardless of *x*. The peak positions in the line profiles seem to agree between Figs. 2(b) and 2(d). Thus, it can be concluded that these peaks indicate the InGaN QDs, and the regions around the valleys between the peaks indicate the GaN, which was deposited as a barrier layer [see the illustration in Fig. 4(c)]. Both the HAADF-STEM intensity and In-L_β intensity are very weak around the positions of 20 and 60 nm, where SiN_x masks might have been placed.

Figure 3 shows nanoanalysis along the line parallel to the *c* axis. The HAADF-STEM intensity shown in Fig. 3(b) increased, as a whole, with the distance from the edge, which can be ascribed to the increase of the specimen thickness. Although it is difficult to determine what corresponds to all the HAADF-STEM peaks observed, at least we can ascertain that the first peak (around the position of 20 nm) and the last one (around the position of 60 nm) are from the InGaN layers because the In intensities are high, as shown in Fig. 3(d). The width of the space between these InGaN layers is about 40 nm, which is the evaluated thickness for the GaN barrier layer that was deposited at the nominal thickness of 100 nm.

In Fig. 4 are shown the two cross-sectional highly magnified HAADF-STEM images near the specimen edge. The line indicated by the arrowhead in Fig. 4(a) or 4(b) is the projection of a SiN_x layer, where SiN_x mask islands were

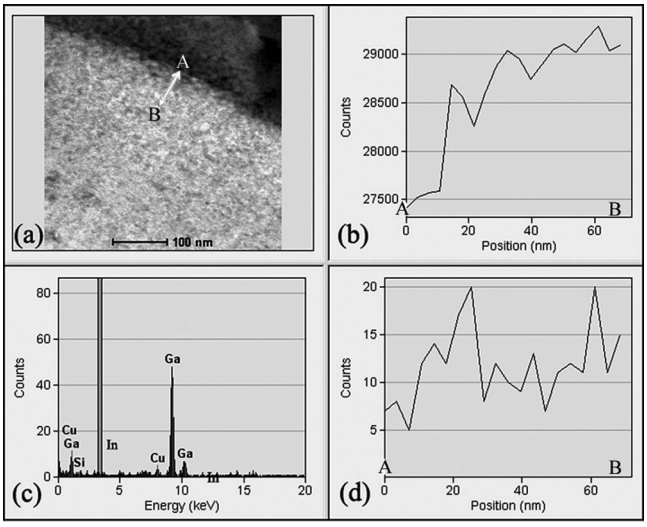

FIG. 3. (a) HAADF-STEM image in which the area line scanned for EDX is indicated. (b) HAADF-STEM intensity profile along the line *A*-*B* shown in (a). (c) EDX spectrum. (d) Indium L_β intensity profile along the line *A*-*B* in (a).

deposited on the (0001) plane of the underlying GaN barrier layer. The dark contrast of the line is due to the small thermal diffuse scattering cross section of Si[14] (and N[7]). The nanoanalysis shown in Fig. 2 was performed along the area around this line. From the thickness of the dark line, the height of the SiN_x masks is roughly estimated to be less than 2 nm.

The bright triangles marked by Q in Fig. 4(b), which resemble peaks in a mountain chain, should be InGaN QDs. The height of the QDs is estimated to be several nanometers, which is not in disagreement with the results from Tu *et al.*[17] The edges of the triangles could be the $\{10\bar{1}1\}$ surfaces of the QDs. Recently, Shiojiri *et al.*[20] proposed an explanation for the formation of V defects, which are formed in multiple InGaN/GaN QW layers grown at temperatures as low as 800–850 °C. These V defects, which are empty pyramidal pits with a thin six-walled structure with InGaN/GaN $\{10\bar{1}1\}$ QWs, often nucleate on threading dislocations (TDs) crossed with the InGaN QWs just above the underlying GaN:Si layer. It is known that the growth rate of the $\{10\bar{1}1\}$ surfaces of GaN crystals decreases with decreasing temperature, while the growth rate of the (0001) surface increases.[21] Shiojiri *et al.* took into account this crystal habit and a masking effect of In atoms, which were trapped and segregated in the strained field around the core of the TD, and then suggested that if a mask disturbing the (0001) layer growth is placed at a low temperature, the resulting crystals exhibit $\{10\bar{1}1\}$ facets. The same mechanism is applicable to the growth of QDs. The InGaN was deposited at the low temperature of 800 °C to avoid the low sticking coefficient of In atoms at high growth temperatures. Then the QDs grew as small island crystals with $\{10\bar{1}1\}$ surfaces due to the masking of the SiN_x, exhibiting natural crystal behavior at the low temperature. The structure of the specimen is schematically shown in Fig. 4(c). The GaN capping layer, deposited at 1000 °C, covered the QDs (and also surfaces of the masks with no deposited QDs) and caused the outermost surface of the specimen to develop with the (0001) plane, accordingly.

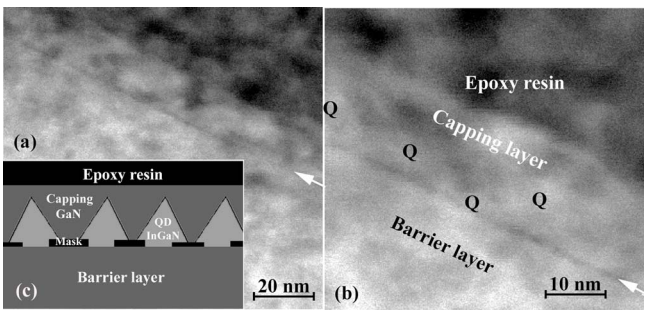

FIG. 4. (a) HAADF-STEM image near the top of the specimen. (b) High-magnified HAADF-STEM image. White arrowheads indicate SiN_x layers. Q, InGaN QDs. (c) Schematic cross section of the specimen.

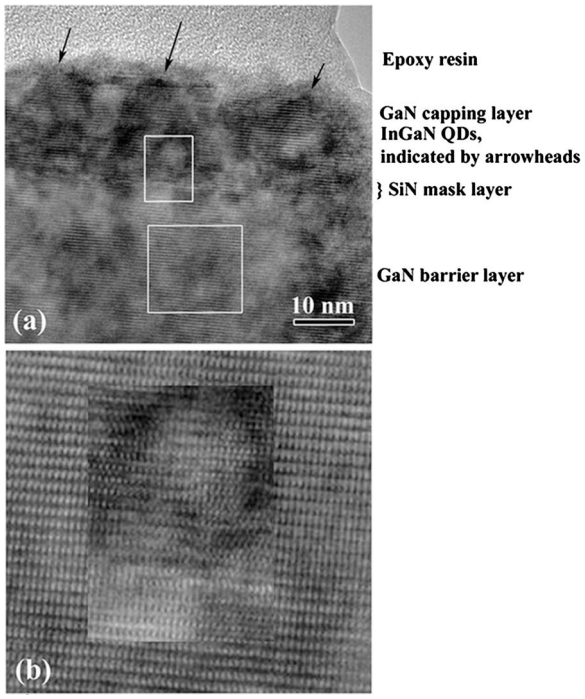

FIG. 5. (a) HRTEM image near the top of the specimen. (b) Enlarged image of the area enclosed by the square in (a), which insets the enlarged image of the area enclosed by the rectangle.

Figure 5(a) shows a HRTEM image near the specimen edge, where part of the capping layer was removed during the ion milling. QDs that are quite high (indicated by arrowheads) are seen on the SiN_x mask layer. The dark contrast may be caused by the diffraction effect of the high structure amplitude of In and the large lattice strain in the QDs. The HRTEM image reveals that the lattices in the QDs were coherently connected with the GaN lattice in the capping layer, although they were strained. The rectangular frame in Fig. 5(a) encloses an area containing the SiN_x layer, and the square frame encloses an area in the GaN barrier layer. In Fig. 5(b), the former area is the inset on the latter area. The images show that the area to be regarded as the SiN_x mask surely has a heavily strained lattice, but they do not allow us to determine the crystal structure or the composition x of the SiN_x.

IV. CONCLUSION

We performed cross-sectional analysis of a sample with three-dimensional (3D) InGaN QDs by high-angle annular dark-field (HAADF) scanning transmission electron microscopy (STEM), high-resolution transmission electron microscopy (HRTEM), and energy dispersive x-ray spectroscopy (EDX). Since the InGaN QDs or InGaN nanosized island crystals were randomly distributed on the masked (0001) surface of the underlying GaN crystal, it was difficult to resolve individual QDs by overlapping, even in the ion-thinned specimen. The following is a summary of the experiment.

(1) The sample consisted of an ultrahigh density of InGaN QDs grown at a reactor temperature of 800 °C on the (0001) surface of an underlying GaN layer that was partially covered with a SiN_x masks. Metal organic vapor phase epitaxy (MOVPE) was used for the sample preparation, and the specimens for cross-sectional EM analysis were prepared by mechanical polishing, followed by ion milling.

(2) The SiN_x masks were confirmed by Si emission in the EDX spectrum and observed as a dark line in HAADF-STEM image. The height of the SiN_x masks was roughly estimated from the thickness of the dark line to be less than 2 nm. In HRTEM images, the SiN_x masks had heavily strained lattices, but the crystal structure and the value of x could not be determined from the lattice image.

(3) The InGaN QDs were observed as bright triangles in the HAAADF-STEM images. The height of the QDs is estimated to be several nanometers. The edges of the triangles, which were the surfaces of the QD, were assumed to be $\{10\bar{1}1\}$ planes by analogy with the behavior of V defects, which form in multiple InGaN/GaN quantum wells deposited at temperatures of 800–850 °C. This HAADF-STEM observation of the InGaN QDs was supported by EDS qualitative nanoanalysis and HRTEM. The lattices of the QDs in the HRTEM images were strained as compared to the underlying and the capping GaN layers.

(4) The GaN capping layer, deposited at 1000 °C, covered the whole QD layer and masks and caused the outermost plane of the specimen to have a (0001) surface. HRTEM observation showed that the lattice in the GaN was very coherently connected with the lattices of the InGaN QDs.

ACKNOWLEDGMENTS

We thank Dr. C. C. Chuo for discussion and also Z. H. Lee for assistance in MOCVD growth, which was financially supported by the Ministry of Economic Affairs of Taiwan, R.O.C., under Project No. 5301XXN300.

[1] S. Nakamura, T. Mukai, M. Senoh, S. Nagahama, and N. Iwasa, J. Appl. Phys. **774**, 3911 (1993).
[2] Y. Narukawa, Y. Kawakami, M. Funato, S. Fujita, S. Fujita, and S. Nakamura, Appl. Phys. Lett. **70**, 981 (1997).
[3] T. Takeuchi, H. Takeuchi, S. Sato, H. Sakai, and H. Amano, Jpn. J. Appl. Phys., Part 2 **36**, L177 (1997).
[4] K. P. O'Donnell, R. W. Martin, and P. G. Middleton, Phys. Rev. Lett. **82**, 237 (1999).
[5] P. Riblet, H. Hirayama, A. Kinoshita, A. Hirata, T. Sugano, and Y. Aoyagi, Appl. Phys. Lett. **75**, 2241 (1999).
[6] K. Watanabe *et al.*, Appl. Phys. Lett. **82**, 715 (2003).
[7] J. M. Gérard, O. Cabrol, and B. Sermage, Appl. Phys. Lett. **68**, 3123 (1996).
[8] S. Keller, B. P. Keller, M. S. Minsky, J. E. Bowers, U. K. Mishra, S. P. DenBaars, and W. Seifert, J. Cryst. Growth **189/190**, 29 (1998).
[9] H. Hirayama, S. Tanaka, P. Ramvall, and Y. Aoyagi, Appl. Phys. Lett. **72**, 1736 (1998).
[10] K. Tachibana, T. Someya, and Y. Arakawa, Appl. Phys. Lett. **74**, 383 (1999).
[11] G. T. Liu, A. Stintz, H. Li, K. J. Malloy, and L. F. Lester, Electron. Lett. **35**, 1163 (1999).
[12] B. Daudin, F. Widmann, G. Feuillet, Y. Samson, M. Arlery, and J. L. Rouvière, Phys. Rev. B **56**, R7069 (1997).
[13] B. Damilano, N. Grandjean, F. Semond, J. Massies, and M. Leroux, Appl. Phys. Lett. **75**, 962 (1999).
[14] B. Damilano, N. Grandjean, S. Dalmasso, and J. Massies, Appl. Phys. Lett. **75**, 3751 (1999).
[15] C. Adelmann, J. Simon, G. Feuillet, N. T. Pelekanos, and B. Daudin, Appl. Phys. Lett. **76**, 1570 (2000).
[16] S. Tanaka, S. Iwai, and Y. Aoyagi, Appl. Phys. Lett. **69**, 4096 (1996).
[17] R. C. Tu *et al.*, Jpn. J. Appl. Phys., Part 2 **43**, L264 (2004).
[18] S. J. Pennycook and P. D. Nellist, *Impact of Electron and Scanning Probe Microscopy on Material Research* (Kluwer, Dordrecht, 1999), pp. 161–207.
[19] M. Shiojiri and H. Saijo, J. Microsc. **223**, 172 (2006).
[20] M. Shiojiri, C. C. Chuo, J. T. Hsu, J. R. Yang, and H. Saijo, J. Appl. Phys. **99**, 073505 (2006).
[21] K. Hiramatsu, K. Nishiyama, A. Motogaito, H. Miyake, Y. Iyechika, and T. Maeda, Phys. Status Solidi A **176**, 535 (1999).